

Extending Fermi-LAT and H.E.S.S. Limits on Gamma-ray Lines from Dark Matter Annihilation

Stefano Profumo^{1*}, Farinaldo S. Queiroz^{2†}, Carlos E. Yaguna^{2‡}

¹ *Department of Physics, University of California, Santa Cruz
Santa Cruz Institute for Particle Physics, 1156 High St, Santa Cruz, CA 95064*

² *Max-Planck-Institut für Kernphysik,
Saupfercheckweg 1, 69117 Heidelberg, Germany*

Abstract

Gamma-ray lines from dark matter annihilation ($\chi\chi \rightarrow \gamma X$, where $X = \gamma, h, Z$) are always accompanied, at lower energies, by a continuum gamma-ray spectrum stemming both from radiative corrections ($X = \gamma$) and from the decay debris of the second particle possibly present in the final state ($X = h, Z$). This model-independent gamma-ray emission can be exploited to derive novel limits on gamma-ray lines that do not rely on the line-feature. Although such limits are not expected to be as stringent, they can be used to probe the existence of γ -ray lines for dark matter masses beyond the largest energies accessible to current telescopes. Here, we use continuous gamma-ray searches from Fermi-LAT observations of Milky Way dwarf spheroidal galaxies and from H.E.S.S. observations of the Galactic Halo to extend the limits on the annihilation cross sections into monochromatic photons to dark matter masses well beyond 500 GeV (Fermi-LAT) and 20 TeV (H.E.S.S.). In this large mass regime, our results provide the first constraints on γ -ray lines from dark matter annihilation.

Key words: astroparticle physics; gamma-rays: general; gamma-rays: galaxies; line: identification; (cosmology:) dark matter

1 Introduction

Indirect searches for dark matter are one of the most promising ways to detect the dark matter particle and to determine its fundamental proper-

*profumo@ucsc.edu

†farinaldo.queiroz@mpi-hd.mpg.de

‡carlos.yaguna@mpi-hd.mpg.de

ties Buckley et al. (2013). Indirect signatures include searches for anomalous γ , ν , e^+ and \bar{p} emission produced by dark matter annihilation in astrophysical objects that could be observed over, and disentangled from, the expected backgrounds from known astrophysical emission. Gamma-ray searches Bringmann & Weniger (2012), in particular, currently provide some of the most stringent and robust constraints on the dark matter annihilation cross section into different final states Cirelli (2015).

These searches can be generically divided into three different categories:

(i) Prompt continuum emission, ranging from $E \sim M_{DM}$ down to soft gamma-ray energies, from dark matter annihilation into any SM final state (e.g. $b\bar{b}$ or W^+W^-) radiating photons, and/or producing photons as a result of hadronization of the decay products of the final-state particles (for example $\pi^0 \rightarrow \gamma\gamma$);

(ii) Secondary continuum emission, resulting from the radiative processes associated with stable, charged particles produced in the annihilation event (such as electrons and positrons); this emission extends from radio all the way to gamma-ray frequencies (see e.g. Colafrancesco et al. (2006, 2007) and Ref. Profumo & Ullio (2010) for a review)

(iii) Monochromatic (line-like) photon emission, resulting from two-body final states containing a photon, for example $\gamma\gamma$, γZ , and γh , or from internal Bremsstrahlung Bergstrom et al. (2005a,c,b); Bringmann et al. (2008, 2011).

While the continuum emission expected from (i) and (ii) can have morphological and spectral features that would enable distinguishing a dark matter component from astrophysical diffuse emission, lines in the GeV–TeV energy range, especially if accompanied by an extended morphology¹ Carlson et al. (2013) can be unmistakably associated with dark matter annihilation (or decay). As a result, current limits on the dark matter annihilation cross section into monochromatic photons are often more constraining than those from continuum emissions².

At a dark matter mass (M_{DM}) of 100 GeV, for example, the Fermi-LAT constraint on $\sigma v(\chi\chi \rightarrow \gamma\gamma)$ –denoted in the following by $\sigma v_{\gamma\gamma}$ – is almost three orders of magnitude stronger than that on $\sigma v(\chi\chi \rightarrow b\bar{b})$ Ackermann et al. (2015a,b). But while the Fermi-LAT limits on $\sigma v(\chi\chi \rightarrow b\bar{b})$ extend all the way up to dark matter masses of 10 TeV, the limits on $\sigma v_{\gamma\gamma}$ are restricted to $M_{DM} < 500$ GeV, which corresponds to the largest photon energy probed by Fermi-LAT collaboration in their spectral line Ackermann et al. (2015b). A similar effect occurs in the H.E.S.S. telescope beyond 20 TeV. Hence, we will refer to those energies as the detectors energy limit.

Consequently, Fermi-LAT data do not provide, at face value, limits on

¹Cold pulsar winds can produce gamma-ray lines, but are point-like sources Aharonian et al. (2012).

²On the other hand, the pair-annihilation cross section of dark matter to two-body final states including a photon is generically suppressed by requiring the dark matter to be essentially electrically neutral.

$\sigma v_{\gamma\gamma}$ for dark matter masses beyond 500 GeV. Similarly, H.E.S.S. data can only constrain $\sigma v_{\gamma\gamma}$ for dark matter masses smaller than about 20 TeV Abramowski et al. (2013). In other words, the energy upper limit corresponds to the maximal dark matter mass probed by these telescopes in the search for gamma-ray lines.

Monochromatic photons from dark matter annihilation, however, always produce a continuum gamma-ray spectrum that extends down to low energies. This model-independent spectrum is generated either by radiative emission Ciafaloni et al. (2011) (for $\gamma\gamma$) or by the decay of the particle accompanying the photon (for γZ and γh). By exploiting this continuum spectrum, bounds on $\sigma v_{\gamma\gamma}$, $\sigma v_{\gamma Z}$ and $\sigma v_{\gamma h}$ may be derived even for dark matter masses much larger than the energy upper limit of a given gamma-ray telescope. This simple observation, which seems to have been overlooked in the previous literature, is the basis of our work.

Although the bounds derived from this continuum spectrum are not expected to be as stringent as those based on the line-feature, they allow to extend the limits on gamma-ray lines from dark matter annihilation to masses not previously testable due to the energy range of the telescopes. In this way, available experimental data can be used to constrain in a novel and independent way the fundamental properties of the dark matter particle Yaguna (2009).

As an example, consider a 1 TeV dark matter particle pair-annihilating into photon pairs with a 100% branching ratio. At first sight, Fermi-LAT seems to have no sensitivity to such a scenario because the signal –a γ -ray line with $E_\gamma = 1$ TeV– lies above the Fermi-LAT energy limit. But, the final state photons may radiate, via weak corrections, W^\pm gauge bosons that will in turn give rise to a gamma-ray continuum emission within the Fermi-LAT energy range. Thus, thanks to the continuum emission associated with the lines, Fermi-LAT becomes sensitive to such a dark matter particle.

Here, we apply this idea to both Fermi-LAT and H.E.S.S. limits on continuum emission from dark matter. Specifically, we use Fermi-LAT observations of dwarf spheroidal galaxies using PASS 8 class of events Ackermann et al. (2015a) to set limits on $\sigma v_{\gamma\gamma}$, $\sigma v_{\gamma Z}$ and $\sigma v_{\gamma h}$ for dark matter masses above 500 GeV, and H.E.S.S. observations of the Galactic center region Abramowski et al. (2011) to extend the range of limits on γ -ray lines to dark matter masses beyond 20 TeV. In this mass range, our results provide the first, model-independent constraints on γ -ray lines from dark matter annihilations.

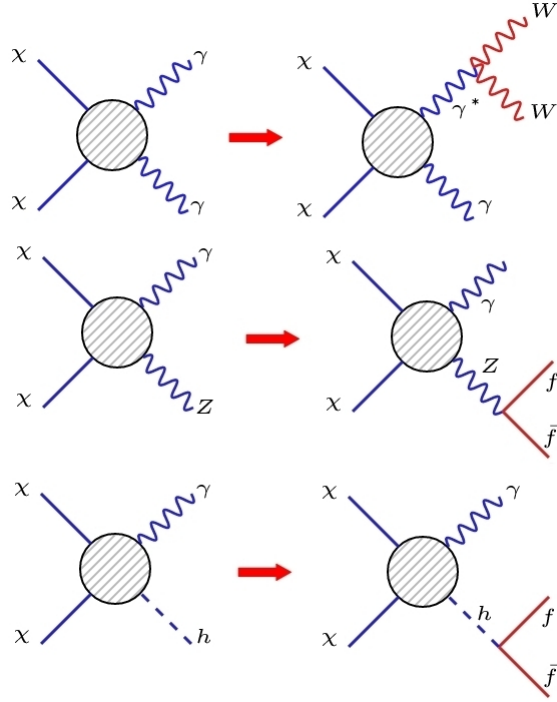


Figure 1: Diagrams illustrating how a continuous gamma-ray emission arises from annihilation into gamma-ray lines. We acknowledge the use of the online tool available at <http://feynman.aivazis.com/>

2 Continuum emission associated with gamma-ray lines

Gamma-ray lines from dark matter annihilation are always accompanied by a continuum spectrum at lower energies. For the γZ and γh final states, this spectrum arises mostly from the decay (and subsequent hadronization of the decay products) of the Z and h produced in association with the photons. For the $\gamma\gamma$ final state, a continuum emission stems from radiative corrections from QED and weak interactions Ciafaloni et al. (2011). A final state photon may, for instance, radiate W bosons (see figure 1), which eventually decay producing a well-known continuum gamma-ray spectrum. For the γZ and γh final states this lower-energy gamma-ray emission is more pronounced since both Z and h decays lead to sizable continuum gamma-ray emissions, as exemplified in Fig.1.

It is important to note that the continuum spectrum associated with γ -ray lines is model-independent, for it arises entirely from Standard Model physics. Therefore, such a spectrum can be used to probe the existence of the primary annihilation channel containing the photon. Here, we use the

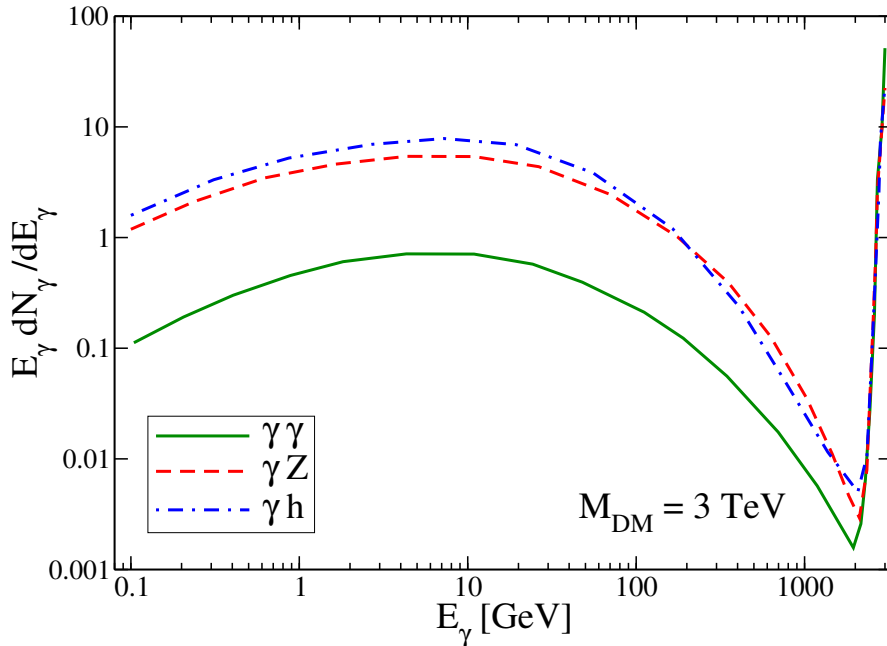


Figure 2: The continuum spectrum associated with gamma-ray lines for a dark matter mass of 3 TeV. The primary annihilation channel is assumed to be $\gamma\gamma$ (solid blue line), γZ (dashed orange line), or γh (dash-dotted green line).

gamma-ray fluxes as incorporated into the PPPC Code Cirelli et al. (2011), which already include the relevant electroweak corrections Ciafaloni et al. (2011).

For the sake of illustration, we show, in figure 2, the continuum spectrum from the annihilation of dark matter into final states containing one or two monochromatic photons. The dark matter mass is assumed in the figure to be 3 TeV, whereas the primary annihilation channels were taken to be $\gamma\gamma$ (solid green line), γZ (dashed red line), or γh (dash-dotted blue line, with h assumed to be a purely Standard Model-like Higgs). Notice that the shape of the spectrum is similar for all three channels but, as expected, the γZ and γh final states produce many more photons than the $\gamma\gamma$ one, which is generically suppressed by factors of order $\sim \alpha_2 \ln^2 M_{DM}^2 / M_W^2$ Ciafaloni et al. (2011). For this particular dark matter mass, the difference between the $\gamma\gamma$ continuum emission and that from γZ and γh amounts to one order of magnitude at most. The γZ and γh final states give rise to relatively similar spectra due to the similar gamma-ray yield resulting from the Z and h decays.

For dark matter annihilating into monochromatic photons, the differen-

tial flux of photons from a given angular direction $\Delta\Omega$ is given by

$$\frac{d\Phi_\gamma(\Delta\Omega)}{dE}(E_\gamma) = \frac{1}{4\pi} \frac{\sigma v_{\gamma X}}{2M_{DM}^2} \frac{dN_\gamma}{dE_\gamma} \cdot J_{ann} \quad (1)$$

where J_{ann} is the annihilation J-factor,

$$J_{ann} = \int_{\Delta\Omega} d\Omega \int \rho_{DM}(s) ds \quad , \quad s = s(\theta) \quad , \quad (2)$$

where ρ_{DM} is the dark matter density which is assumed be well described by a NFW profile,

$$\rho_{DM}(r) = \frac{\rho_s}{r/r_s(1+r/r_s)} \quad . \quad (3)$$

where ρ_s and r_s are the characteristic density and scale radius determined dynamically from the maximum circular velocity v_c and the enclosed mass contained up to the radius of maximum v_c as discussed in Ackermann et al. (2014). The integral is performed over the line of sight element within the solid angle $\Delta\Omega$. In this work we adopted the J-factors listed in the table I of Ackermann et al. (2015a) which is equivalent to Ackermann et al. (2014). As for $\frac{dN_\gamma}{dE_\gamma}$ is the differential γ -ray yield per annihilation into the final state γX , with $X = \gamma, Z, h$. Since this yield is model-independent –see figure 2– gamma-ray data can be used to constrain regions in the plane M_{DM} vs $\sigma v_{\gamma X}$.

In our analysis we derive limits from Fermi-LAT and H.E.S.S. data.

3 Fermi-LAT limits

The Fermi-LAT telescope has observed a wealth of dwarf spheroidal satellite galaxies of the Milky Way, which are known to be dark matter-dominated objects. The resulting data belonging to the P8R2SOURCEV6 event class, based on six years of observations, span energies between 500 MeV and 500 GeV. The collaboration makes use of the Pass-8 software which results into an improved point spread function and effective area compared to previous releases and includes the third point source Fermi-LAT catalog (3FGL). Since none of the dwarf galaxies presents any significant gamma-ray excess, tight constraints on the dark matter annihilation cross section can be placed Ackermann et al. (2015a) –see also Ahnen et al. (2016,?); Oman et al. (2016); Li et al. (2016); Dutta et al. (2015); Zitzer (2015); Rico et al. (2015); Bonnard et al. (2015b,a); Hooper & Linden (2015); Geringer-Sameth et al. (2015); Drlica-Wagner et al. (2015); Baring et al. (2016); Queiroz et al. (2016).

Fermi-LAT has made publicly available³ binned Poisson maximum-likelihood tools that can be used to reproduce the individual limits stemming from any

³http://www-glast.stanford.edu/pub_data/1048/

of the dwarf galaxies in the study, without accounting for uncertainties on the J-factors of each dwarf galaxy, assumed to be described by a NFW dark matter density profile. Here we perform a joint likelihood analysis across the 15 dwarf galaxies, and treat the J-factor as a nuisance parameter, following the recipe described in the supplemental material of Ref. Ackermann et al. (2015a). In doing so, we use the likelihood of an individual dwarf i , defined as,

$$\tilde{\mathcal{L}}_i(\mu, \theta_i = \{\alpha_i, J_i\} | D_i) = \mathcal{L}_i(\mu, \theta_i | D_i) \mathcal{L}_J(J_i | J_{obs,i}, \sigma_i) \quad (4)$$

where μ encompasses the parameters of the DM model, i.e. the ratio of the dark matter annihilation cross section and mass, whereas θ_i refers for the set of nuisance parameters from the LAT analysis (α_i) and J-factors of the dwarf galaxies J_i , with D_i being the gamma-ray data. The former is provide by the Fermi-LAT team as mentioned. In order to account for the statistical uncertainties on the J-factors of each dwarf galaxy, a J-factor likelihood function is defined as follows,

$$\begin{aligned} \mathcal{L}_J(J_i | J_{obs,i}, \sigma_i) &= \frac{1}{\ln(10) J_{obs,i} \sqrt{2\pi} \sigma_i} \\ &\times \exp \left\{ -\frac{(\log_{10}(J_i) - \log_{10}(j_{obs,i}))^2}{2\sigma_i^2} \right\} \end{aligned}$$

where J_i is referred as the true value of the J-factor of a dwarf galaxy i , whereas $J_{obs,i}$ is the measured J-factor with error labelled as σ_i . Then we join the likelihood terms,

$$\mathcal{L}_i(\mu, \theta_i | D_i) = \prod_j \mathcal{L}_i(\mu, \theta_i | D_{i,j}) \quad (5)$$

and perform a test statistic (TS), with $TS = -2\ln(\mathcal{L}(\mu_0, \hat{\theta} | D) / \mathcal{L}(\hat{\mu}, \hat{\theta} | D))$, which gives rise to 95% C.L. upper limit on the energy flux as explained in Rolke et al. (2005) by imposing a change in the log-likelihood of $= 2.71/2$ from its maximum. In order to demonstrate that our results are solid, we reproduced Fermi-LAT limits from the usual channels finding a very good agreement. See figure 3 where we show that explicitly for the W^+W^- channel.

With the maximum likelihood at hand, we feed a given gamma-ray spectrum, here the low-energy continuum from $\gamma\gamma, \gamma Z$ and γh , and we obtain a bound on the annihilation cross section arising from the gamma-ray continuum emission from a stack of 15 dwarfs.

Our results are summarized in Fig. 4. It shows the 95% C.L. limits on the thermally averaged, zero-temperature pair-annihilation cross section to γX , for $X = \gamma, Z, h$. As previously discussed, the annihilation final states γZ and γh yield similar gamma-ray emission, and consequently nearly equivalent

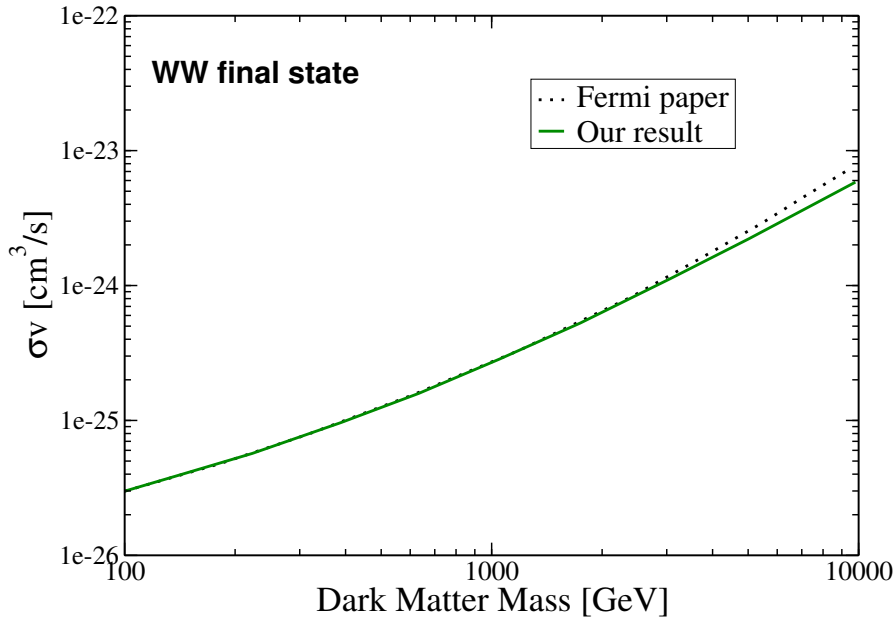


Figure 3: Comparison between Fermi-LAT official limit and ours for annihilation into WW. It is clear that our limits have a very good agreement with the official limits from Fermi-LAT. Similar conclusions are found for all channels.

limits, whereas pure annihilation into photon pair is less constraining due to the lower associated continuum emission level. For reference, we display in this figure the current bounds on gamma-ray lines reported by the Fermi-LAT Ackermann et al. (2015b) and H.E.S.S. collaborations (dotted black lines).

In addition, the unitarity bound on the size of the pair-annihilation cross section Griest & Kamionkowski (1990) (dashed black line) is also shown. This bound, derived via partial-wave unitarity, sets a model-independent upper limit on the annihilation rate of the dark matter particles. Today, this upper limit amounts, for s-wave annihilation, to $\sigma v \sim \frac{1.5 \times 10^{-13} \text{cm}^3 \text{s}^{-1}}{(\text{GeV}/m_{DM})^2}$ Beacom et al. (2007), where $v \approx 10^{-3}$ was used for the velocity of the dark matter particles. Only the region below the dashed black line is thus consistent with unitarity.

Our new limits, though not as stringent as those based on the line-feature, provide the first Fermi-LAT constraints on gamma-ray lines from dark matter annihilation for $M_{DM} > 500$ GeV. Even if these limits are weaker than (or consistent with) the current H.E.S.S. limits Abramowski et al. (2013), they constitute a new and independent limit on gamma-ray lines that is based on a different astrophysical target and that relies entirely on Fermi-LAT data.

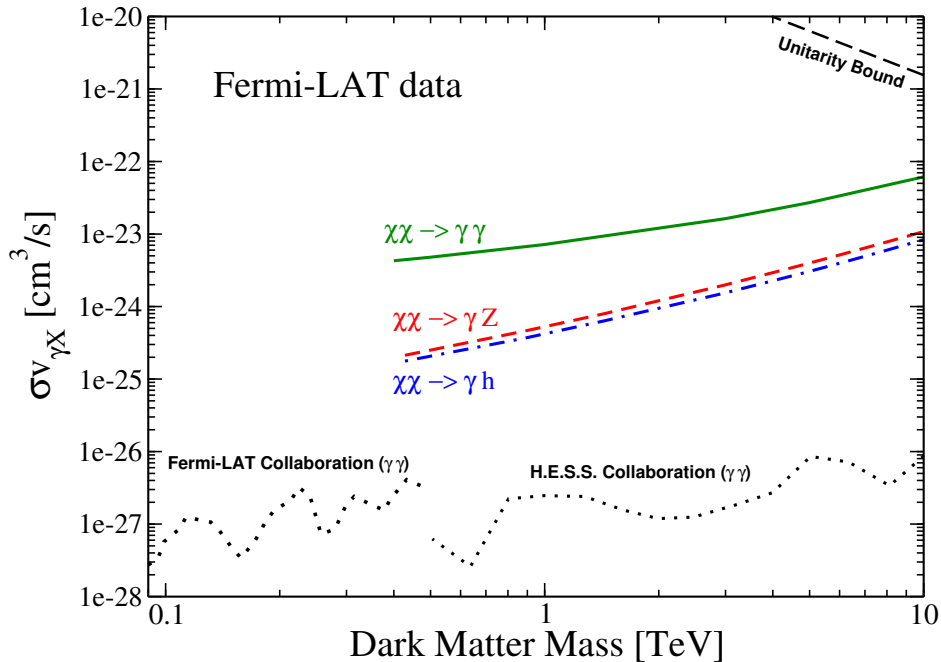


Figure 4: Limits on γ -ray lines from dark matter annihilation derived from Fermi-LAT data. The colored lines show our results –based on the continuum spectrum and using observations of dwarf galaxies– for different cross sections: $\sigma v_{\gamma\gamma}$ (solid green line), $\sigma v_{\gamma Z}$ (dashed red line), and $\sigma v_{\gamma h}$ (dash-dotted line). The dotted black line shows instead the limits derived by the Fermi-LAT collaboration Ackermann et al. (2013)–based on the line-feature and using data from the region around the Galactic center. For reference, the unitarity bound on s-wave annihilation cross sections is also shown (dashed black line; see Ref. Griest & Kamionkowski (1990) for details on the unitarity bound and the associated assumptions).

4 H.E.S.S. limits

In Abramowski et al. (2011), the H.E.S.S. collaboration presented their latest results on the search for a dark matter annihilation signal from the Galactic Center Halo, which are based on 112 hours of GC observations taken over a period of about four years. In their analysis, H.E.S.S. divides the sky into background and source regions, with the former located further away from the Galactic plane, where a dark matter signal is expected to be dimmer. The source region used in Abramowski et al. (2011) was a circular region of radius 1° from which Galactic latitudes $|b| < 0.3^\circ$ were removed to reduce the possible contamination of the dark matter signal by local γ -ray sources. Since no excess emission was found by H.E.S.S., restrictive limits were placed on the dark matter annihilation cross section, which are among the most stringent for dark matter masses above ~ 800 GeV.

By integrating Fig.3 of Ref. Abramowski et al. (2011) multiplied by ob-

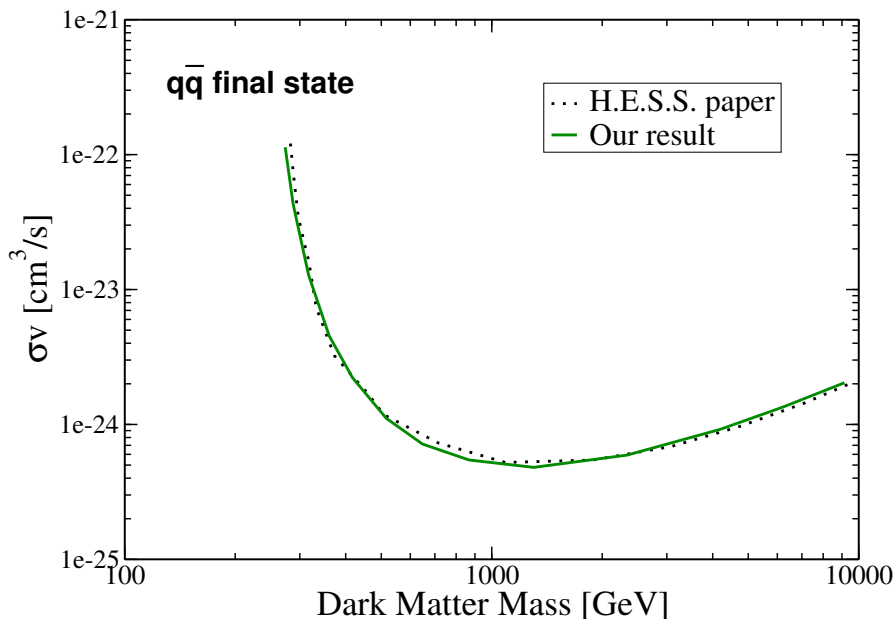


Figure 5: Comparison between H.E.S.S. official limit and ours for annihilation into quarks using the parametric spectrum defined in Hill et al. (1987); Tasitsiomi & Olinto (2002). This parametric energy spectrum includes dark matter annihilation into all quark flavors. Our results strongly overlap proving the robustness of our analysis.

servation time, effective area, and J-factor we can compute the number of signal events for the ON (N^{SON}) and OFF (N^{SOFF}) regions as well as the number of background (N^B) events for the OFF regions. ON region refers to the 1° circular region around the Galactic Center, whereas the OFF regions are represented by annulus of radii of 1° and 1.5° as delimited in Fig.2 of Abramowski et al. (2011)⁴. We can then define likelihood functions as described in Lefranc & Moulin (2015) and compute 95% C.L. limits similarly to the procedure discussed for Fermi-LAT. In Fig.5 for concreteness we compare our limit with the one obtained by H.E.S.S. collaboration. The limits are for dark matter annihilations into all quarks using the parametric energy spectrum as defined in Hill et al. (1987); Tasitsiomi & Olinto (2002). From Fig.5 it is clear that our analysis finds a very good agreement with H.E.S.S. result.

After this cross-check, we computed the 95% C.L. bound on annihilation cross section vs dark matter mass plane for the channels $\gamma Z, \gamma h$ and $\gamma\gamma$,

⁴The J-factors are given in the H.E.S.S. paper and the effective area was obtained using the code `gammapy` code <https://gammapy.readthedocs.io/en/latest/>, which offers quite good agreement with the effective area made public in several PhD thesis from H.E.S.S. members (e.g. <https://www.physik.hu-berlin.de/de/eophys/HESS/theses/pdfs/ArneThesis.pdf>)

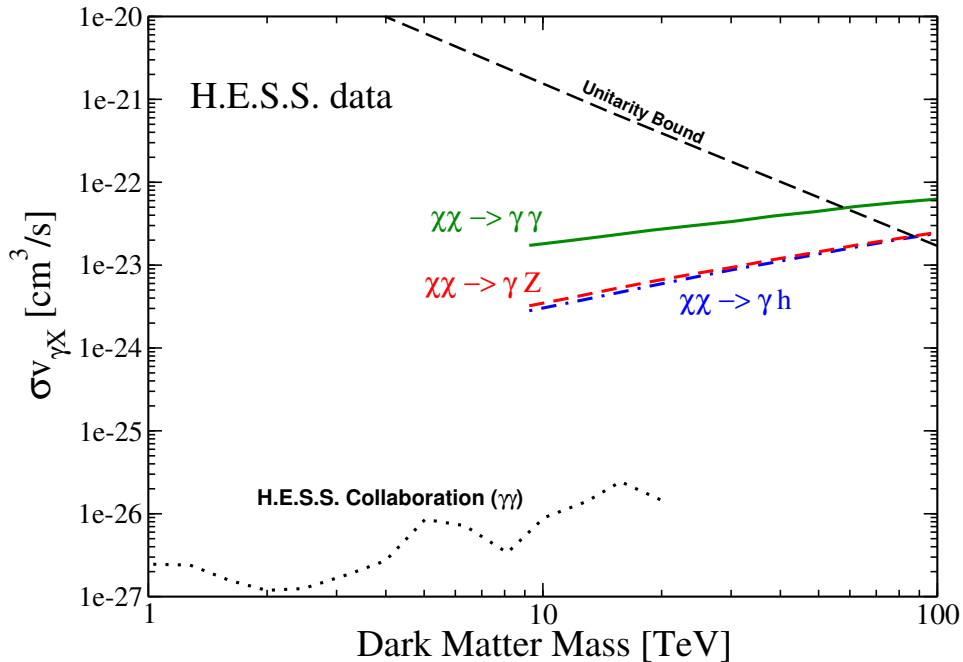


Figure 6: Limits on γ -ray lines from dark matter annihilation derived from H.E.S.S. data. The colored lines show our results –based on the continuum spectrum and using observations of the Galactic center halo– for different cross sections: $\sigma v_{\gamma\gamma}$ (solid green line), $\sigma v_{\gamma Z}$ (dashed red line), and $\sigma v_{\gamma h}$ (dash-dotted line). The dotted black line shows instead the limits derived by the H.E.S.S. collaboration –based on the line-feature and using data from the region around the Galactic center Abramowski et al. (2013). For reference, the unitarity bound on the annihilation cross section is also shown (dashed black line).

using a NFW profile, similarly to Abramowski et al. (2011). Our results are summarized in Fig. 6. Since a 100 TeV dark matter particle annihilating into $\gamma\gamma$ still produces some appreciable amount of continuum gamma-rays below 20 TeV, H.E.S.S. can still probe the properties of such a dark matter particle. To the best of our knowledge, these are the first limits on gamma-ray lines from dark matter annihilation for $M_{DM} > 20$ TeV.

While the new limits we have derived, both from Fermi-LAT and H.E.S.S., on the dark matter annihilation cross sections into monochromatic photons are above the typical cross sections needed to produce dark matter in the early universe as a thermal relic, they are applicable for example to dark matter models where the production mechanism is non-thermal Gelmini et al. (2006), or where a modified expansion rate occurs at the time of decoupling (see e.g. Profumo & Ullio (2003) and references therein). These two possibilities are especially interesting in the large-mass region that our limits cover.

5 Conclusions

In this study we demonstrated that the continuum spectrum associated with γ -ray lines from dark matter annihilation can be used, in conjunction with currently available data, to set new constraints on the dark annihilation cross section into monochromatic photons over a very broad range of dark matter particle masses. This continuum spectrum is model independent, and arises from radiative corrections or from the decay of the particle accompanying the photon –a Higgs boson or a Z . Using limits from six years of Fermi-LAT observations of local dwarf galaxies with PASS-8, we extended current Fermi-LAT limits on $\sigma v_{\gamma\gamma}$, $\sigma v_{\gamma Z}$ and $\sigma v_{\gamma h}$ to dark matter masses well beyond 500 GeV (Fermi-LAT energy upper limit); similarly, using H.E.S.S. observations of the Galactic Halo, we extended the corresponding H.E.S.S. limits to dark matter masses larger than 20 TeV. At these very large masses, our limits provide the first constraints on gamma-ray lines from dark matter annihilation.

Acknowledgements

We thank Fermi-LAT Collaboration for the public data and tools used in this work. We are also grateful to the PPPC team for making their code publicly available. We thank Christoph Weniger for discussions. CY is supported by the Max Planck Society in the project MANITOP. SP is partly supported by the US Department of Energy, Contract DE-SC0010107-001.

References

- Abramowski A., et al., 2011, Phys. Rev. Lett., 106, 161301
- Abramowski A., et al., 2013, Phys. Rev. Lett., 110, 041301
- Ackermann M., et al., 2013, Phys. Rev., D88, 082002
- Ackermann M., et al., 2014, Phys.Rev., D89, 042001
- Ackermann M., et al., 2015a, Phys. Rev. Lett., 115, 231301
- Ackermann M., et al., 2015b, Phys. Rev., D91, 122002
- Aharonian F., Khangulyan D., Malyshev D., 2012, Astron. Astrophys., 547, A114
- Ahnen M. L., et al., 2016, JCAP, 1602, 039
- Baring M. G., Ghosh T., Queiroz F. S., Sinha K., 2016, Phys. Rev., D93, 103009

Beacom J. F., Bell N. F., Mack G. D., 2007, *Phys. Rev. Lett.*, 99, 231301

Bergstrom L., Bringmann T., Eriksson M., Gustafsson M., 2005a, *Phys. Rev. Lett.*, 94, 131301

Bergstrom L., Bringmann T., Eriksson M., Gustafsson M., 2005b, *Phys. Rev. Lett.*, 95, 241301

Bergstrom L., Bringmann T., Eriksson M., Gustafsson M., 2005c, *JCAP*, 0504, 004

Bonnivard V., et al., 2015a, *Mon. Not. Roy. Astron. Soc.*, 453, 849

Bonnivard V., et al., 2015b, *Astrophys. J.*, 808, L36

Bringmann T., Weniger C., 2012, *Phys. Dark Univ.*, 1, 194

Bringmann T., Bergstrom L., Edsjo J., 2008, *JHEP*, 01, 049

Bringmann T., Calore F., Vertongen G., Weniger C., 2011, *Phys. Rev.*, D84, 103525

Buckley J., et al., 2013, in *Community Summer Study 2013: Snowmass on the Mississippi (CSS2013)* Minneapolis, MN, USA, July 29-August 6, 2013. ([arXiv:1310.7040](https://arxiv.org/abs/1310.7040)), <http://inspirehep.net/record/1262275/files/arXiv:1310.7040.pdf>

Carlson E., Linden T., Profumo S., Weniger C., 2013, *Phys. Rev.*, D88, 043006

Ciafaloni P., Comelli D., Riotto A., Sala F., Strumia A., Urbano A., 2011, *JCAP*, 1103, 019

Cirelli M., 2015, 1511.02031

Cirelli M., et al., 2011, *JCAP*, 1103, 051

Colafrancesco S., Profumo S., Ullio P., 2006, *Astron. Astrophys.*, 455, 21

Colafrancesco S., Profumo S., Ullio P., 2007, *Phys. Rev.*, D75, 023513

Drlica-Wagner A., et al., 2015, *Astrophys. J.*, 809, L4

Dutta B., Gao Y., Ghosh T., Strigari L. E., 2015, *Phys. Rev.*, D92, 075019

Gelmini G., Gondolo P., Soldatenko A., Yaguna C. E., 2006, *Phys. Rev.*, D74, 083514

Geringer-Sameth A., Walker M. G., Koushiappas S. M., Koposov S. E., Belokurov V., Torrealba G., Evans N. W., 2015, *Phys. Rev. Lett.*, 115, 081101

Griest K., Kamionkowski M., 1990, Phys.Rev.Lett., 64, 615

Hill C. T., Schramm D. N., Walker T. P., 1987, Phys. Rev., D36, 1007

Hooper D., Linden T., 2015, JCAP, 1509, 016

Lefranc V., Moulin E., 2015, in Proceedings, 34th International Cosmic Ray Conference (ICRC 2015). (arXiv:1509.04123), <http://inspirehep.net/record/1393231/files/arXiv:1509.04123.pdf>

Li S., et al., 2016, Phys. Rev., D93, 043518

Oman K. A., Navarro J. F., Sales L. V., Fattahi A., Frenk C. S., Sawala T., Schaller M., White S. D. M., 2016, Phys. Rev.

Profumo S., Ullio P., 2003, JCAP, 0311, 006

Profumo S., Ullio P., 2010, 1001.4086

Queiroz F. S., Yaguna C. E., Weniger C., 2016, JCAP, 1605, 050

Rico J., Wood M., Drlica-Wagner A., Aleksić J., 2015, in Proceedings, 34th International Cosmic Ray Conference (ICRC 2015). (arXiv:1508.05827), <http://inspirehep.net/record/1389141/files/arXiv:1508.05827.pdf>

Rolke W. A., Lopez A. M., Conrad J., 2005, Nucl. Instrum. Meth., A551, 493

Tasitsiomi A., Olinto A. V., 2002, Phys. Rev., D66, 083006

Yaguna C. E., 2009, Phys. Rev., D80, 115002

Zitzer B., 2015, in Proceedings, 34th International Cosmic Ray Conference (ICRC 2015). (arXiv:1509.01105), <http://inspirehep.net/record/1391628/files/arXiv:1509.01105.pdf>